Proceedings of the ASME 2010 International Design Engineering Technical Conferences & Computers and Information in Engineering Conference
IDETC/CIE 2010
August 15-18, 2010, Montreal, Quebec, Canada

DETC2010-28668

KINEMATICS ANALYSIS OF THE EXECHON TRIPOD

Matteo Zoppi*, Dimiter Zlatanov, and Rezia Molfino
PMAR Robotics Group
DIMEC
University of Genoa
Genoa, Italy
Email: zoppi@dimec.unige.it

ABSTRACT

The Exechon 5-Axis Parallel Kinematic Machine (PKM) is a successful design created in Sweden and adopted by many producers of machine tools around the world. A new version of the manipulator is being developed as a component of a mobile self-reconfigurable fixture system within an inter-European project. The basic Exechon architecture consists of a 3-degree-of-freedom (dof) parallel mechanism (PM) connected in series with a two- or three-dof spherical wrist. The PM has two UPR (4-dof) legs, constrained to move in a common rotating plane, and an SPR (5-dof) leg. The paper presents the kinematic analysis of both the PM and the hybrid parallel-serial architecture. We describe the complex three-dimensional motion pattern of the PM platform, derive the kinematic equations and provide explicit solutions for the inverse kinematics.

NOMENCLATURE

s_γ, c_γ $\sin\gamma, \cos\gamma$
A, C labels of the RRPR legs
B label of the SPR leg
L generic leg, $L = A, B, C$
ξ_i^L normalized (unit) twist of the i-th joint of the leg L
$\ell(\xi)$ axis of a finite-pitch twist ξ
$\mathbf{k}_i^L$ unit vector parallel to $\ell(\xi_i^L)$
$\mathbf{n}_{12}^L$ unit vector with direction $\mathbf{k}_1^L \times \mathbf{k}_2^L$, $L = A, C$
π_α plane through $\ell(\xi_1^A)$ and normal to $\mathbf{k}_4^A$
π_h plane containing $\ell(\xi_5^B)$ and parallel to $\ell(\xi_4^A)$, $\ell(\xi_4^C)$
$\mathbf{e}_h$ unit vector orthogonal to π_h with the direction of $\mathbf{k}_2^A \times \mathbf{k}_5^B$
P_1^L point on $\ell(\xi_1^L)$ and its common normal with $\ell(\xi_2^L)$, $L = A, C$
P_2^L projection of P_1^L on $\ell(\xi_2^L)$, $L = A, C$
P_4^L projection of P_2^L on $\ell(\xi_4^L)$, $L = A, C$
P_1^B center of the S joint
P_5^B projection of P_1^B on $\ell(\xi_5^B)$
P projection of P_5^B on π_α
O projection of P_1^B on $\ell(\xi_1^A)$
π_e^B plane through P_1^B orthogonal to $\mathbf{k}_5^B$
S point on π_e^B
π_0 plane of $\ell(\xi_1^A)$ and P_1^B; if $P_1^B \in \ell(\xi_1^A)$ any plane of the pencil
α angle between π_α and π_0 positive about $\mathbf{j}_b$
β angle between $\mathbf{k}_5^B$ and $\mathbf{k}_1^A$ positive about $\mathbf{k}_2^A$
h distance of O from π_h with sign according to $\mathbf{e}_h$
$O\mathbf{i}_b\mathbf{j}_b\mathbf{k}_b$ reference frame at O with $\mathbf{i}_b \perp \mathbf{k}_1^A$, $\mathbf{j}_b = \mathbf{k}_1^A$, $\mathbf{k}_b \perp \pi_0$
$P\mathbf{ijk}$ reference frame at P with $\mathbf{i} = \mathbf{k}_2^A$, $\mathbf{j} = \mathbf{k}_5^B$, $\mathbf{k} = \mathbf{e}_h$
h_x, h_z respectively: $\mathbf{i}$ and $\mathbf{k}$ coordinates of S in $(P\mathbf{ijk})$
d^A, d^B, d^C respectively: $\mathbf{j}_b$ coordinate of P_1^A, $\mathbf{i}_b$ coordinate of P_1^B, $\mathbf{j}_b$ coordinate of P_1^C, in $(O\mathbf{i}_b\mathbf{j}_b\mathbf{k}_b)$.
p^A, p^B, p^C respectively: $\mathbf{j}$ coordinate of P_4^A, $\mathbf{i}$ coordinate of P_5^B, $\mathbf{j}$ coordinate of P_4^C, in $(P\mathbf{ijk})$.
h^L distance from $\ell(\xi_4^L)$ to π_h, $L = A, C$, sign according to $\mathbf{e}_h$
l_{12}^L distance between $\ell(\xi_1^L)$ and $\ell(\xi_2^L)$, $L = A, C$
δ^L working mode parameter, $\delta^L = \pm 1$, for leg $L = A, C$
δ_1^B, δ_2^B working mode parameters when the end-effector pose is assigned by S $(= \pm 1)$

*Address all correspondence to this author.

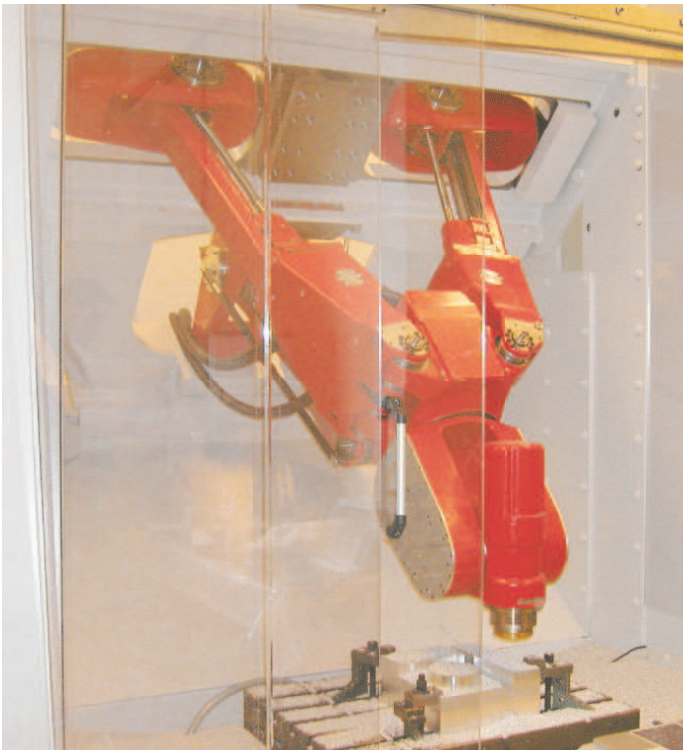

FIGURE 1: THE EXECHON X 700 MODEL.

FIGURE 2: THE EXECHON X 300 MODEL.

1 INTRODUCTION

Parallel Kinematic Machines are machine tools based on parallel mechanisms. PMs are favored because they can provide superior stiffness due to the presence of multiple legs (limbs). This advantage is best exemplified by hexapods such as the Stewart-Gough platform, a popular choice for flight simulators and other applications with requirements for high load-carrying capacity [1]. Unfortunately, a higher number of legs implies a smaller workspace. To achieve a balance, three-legged architectures have been a popular choice for PKM designs. See [2–5]. Although the five dof required in machining applications can be obtained by parallel architectures, [6], hybrid designs with serial wrists are often preferred.

The Tricept developed by Neos Robotics AB, now produced by PKMtricept SL, is a particularly successful example of a tripod for machining applications. A new design, related to the Tricept, is the Exechon tripod, patented in 2006 by Karl-Erik Neumann [7], who had also invented the Tricept in 1985 [8]. Unlike the Tricept, the Exechon tripod has no central stabilizing tube (a passive central leg).

PKMs based on several Exechon designs are now produced in China, Taiwan, Korea, and Spain. Two models can be seen on Figs. 1 and 2. The Exechon 700 and 300 are 5-axis machine tools, more precisely, 3-dof tripods equipped with a 2-dof spherical wrist. A new Exechon variant, with smaller dimensions and a 3-dof spherical wrist, Fig. 3, has been developed for fixturing applications within an inter-European project, SwarmItFIX [9]. The project is to create a self-reconfigurable intelligent fixturing system, primarily intended for the manufacturing of relatively large thin-sheet parts as in the aerospace industry. The envisioned solution uses mobile PMs as autonomous fixturing agents, which periodically reposition to provide support for the machined thin-sheet workpiece in the vicinity of the moving machine tool. The new Exechon X150 model is the centerpiece of the design of the mobile agent.

In this paper we present the kinematics equations of the Exechon tripod, not published previously. We begin by describing the complex three-dimensional motion pattern of the tripod. Then, we formulate and solve the inverse kinematics. Additionally we provide the procedure by which to solve the inverse kinematics for the whole hybrid mechanism when the tripod is combined with a 3-dof wrist.

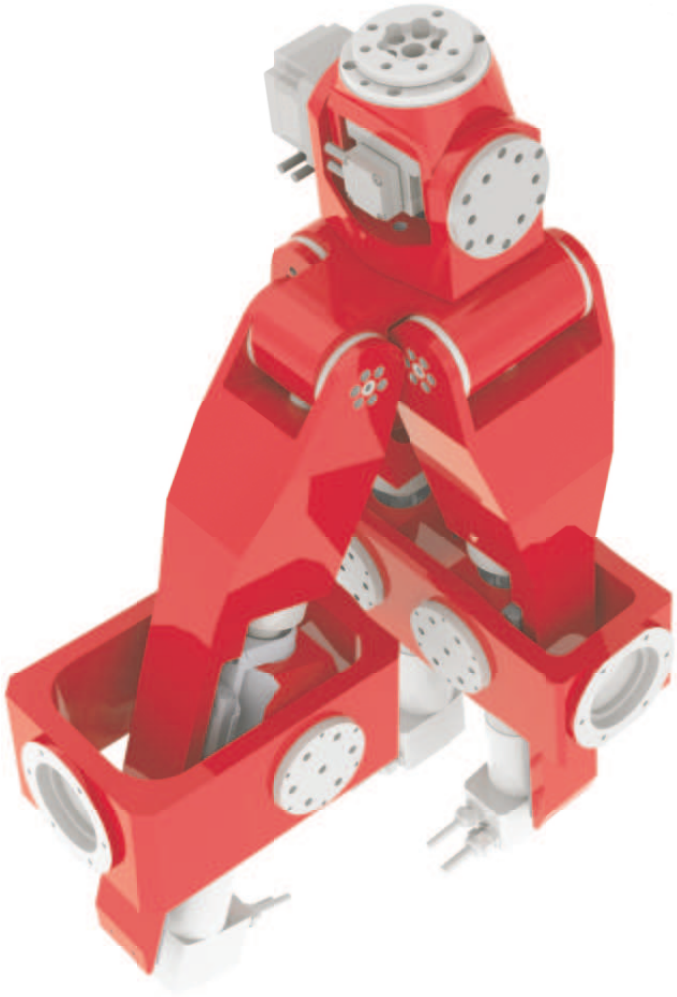

FIGURE 3: THE EXECHON X 150 MODEL.

2 ARCHITECTURE AND GEOMETRY

The parallel mechanism we analyze in this paper is shown in Fig. 4. The notation is summarized in the Nomenclature.

2.1 Architecture

The PM has three legs, herein labeled A, B, C. Two of them, A and C, are identical 4-dof RRP̲R chains. The first joints of these two legs share the same axis: $\ell(\xi_1^A) = \ell(\xi_1^C)$. The remaining revolutes in both legs are all parallel and perpendicular to the two prismatic joints and the first joint axis.

$$\mathbf{k}_3^L \perp \mathbf{k}_4^A \parallel \mathbf{k}_4^C \parallel \mathbf{k}_2^A \parallel \mathbf{k}_2^C \perp \mathbf{k}_1^A \tag{1}$$

Ignoring actuation, each of the A or C legs, as well as the two legs combined, constrain the end-effector of the PM as an RE chain, a revolute followed by a planar joint, with the R axis perpendicular to the normal of the E joint.

For simplicity we will assume that $\mathbf{k}_3^L$ is parallel to the plane of $\ell(\xi_2^L)$ and $\ell(\xi_4^L)$ (if $\ell(\xi_2^L) \neq \ell(\xi_4^L)$), $L = A, C$. This is the case in the existing Exechon designs, where the first two revolutes in each of legs A and C are combined in a universal joint.

The remaining leg, labeled B, is a 5-dof SP̲R serial chain. Its last joint axis, the revolute fixed in the platform is parallel to the planes of planar motion of legs A and C, $\mathbf{k}_5^B \perp \mathbf{k}_4^A$. Furthermore, the direction of the prismatic joint is parallel to the normal from the center of the spherical joint, P_1^B, to the revolute axis, $\ell(\xi_5^B)$. (In the practical Exechon designs, the spherical joint has been sensibly replaced with three revolutes, a U-joint followed by a rotation allowing the leg to twist. For simplicity, and with little loss of generality, we will assume an SPR leg.)

2.2 Geometry

The geometry of a mechanism with the considered architecture is univocally identified by the geometry parameters: d^A, d^B, d^C describing the base of the mechanism; l_{12}^A, l_{12}^C describing legs A and C; p^A, p^B, p^C, h^A, h^C describing the end-effector.

3 MOTION PATTERN

The end-effector has three degrees of freedom which means that its feasible poses form a three-dimensional subspace of $SE(3)$. (Such subspaces are referred to as motion patterns [6] when the interest is in the geometry of the allowed end-effector motion, rather than its limits, the usual subject of workspace analysis.) Indeed, legs A and C constrain the platform to perform planar motion in a rotating plane, i.e. into a four-dimensional submanifold of $SE(3)$. The third leg is with 5 dof, therefore the platform must have at least 3 dof. However, it is clear that not all of the four freedoms permitted by the RE legs are possible, as the 5-dof leg allows translational motion only in directions perpendicular to the platform revolute axis, $\ell(\xi_5^B)$. Thus, not all translations parallel to the plane π_α, allowed by the RE legs A and C, are allowed by leg B. Therefore, the intersection of the motion patterns allowed by the legs is a three-dimensional space.

This means that locally the motion can be described by three parameters. In general, this does not imply that there is a global choice of three parameters describing the pose in a nonsingular manner. (For example, this is not the case for spherical motion; every choice of Euler angles has a singularity.)

However, this is possible for this mechanism. A nonsingular representation is $e = (\alpha, \beta, h)$. The angle α describes the rotation of π_α, the rotating plane of planar motion of legs A and C. The angle β is the planar orientation of the platform in π_α. The third parameter, h, measures how far the platform is translated from the projection of the spherical joint, P_1^C, onto π_α. The

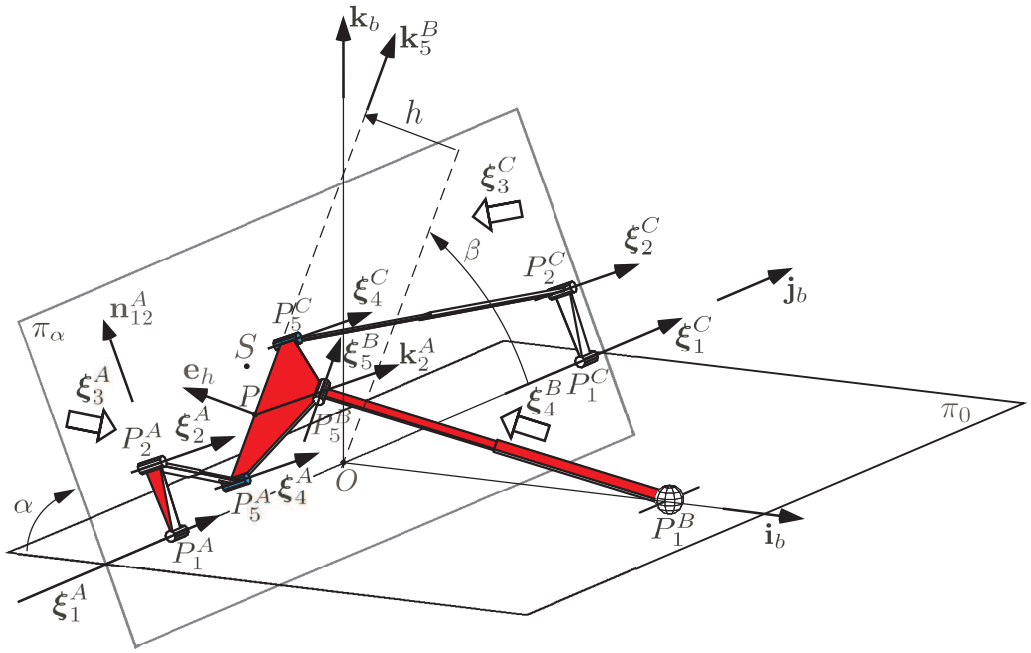

FIGURE 4: GEOMETRY AND CONFIGURATION PARAMETERS

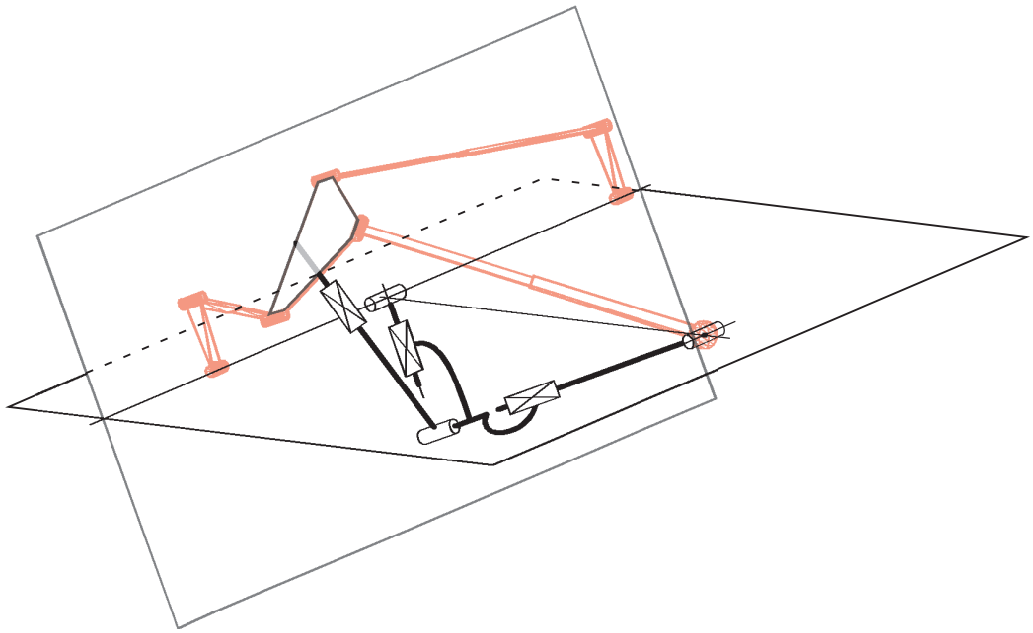

FIGURE 5: THE EQUIVALENT MECHANISM AS A FOURTH LEG.

triple, e, describes the pose of the PM platform univocally for any geometry and configuration.

This does not mean that there exists an RRP serial chain whose end-effector has the same motion pattern as the tripod platform. On the contrary: the second revolute joint in such a hypothetical chain would need to be at the projection of P_1^B, and cannot be fixed at a constant distance from the $\ell(\xi_1^A)$ axis.

However, there is a simple linkage that reproduces exactly the motion pattern of the PM, Figs. 5 and 6. It can be described as a serial chain with three joints, with its first "joint" realized by

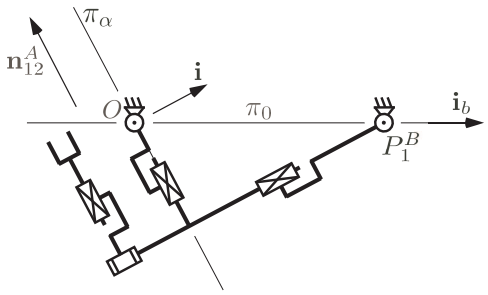

FIGURE 6: THE EQUIVALENT MECHANISM.

a 1-dof 2-RP planar parallel mechanism, while the second and third joints are a revolute and prismatic pair, respectively. The first 1-dof coupling is between the base link and the "coupler" of a four-joint single-loop planar mechanism, Fig. 6. The second revolute joint reproduces exactly the change of the parameter β, and its axis is always along the perpendicular from P_1^B to π_α, while the third provides the translation measured by h (for fixed α and β). Although the configuration of the first complex joint can be described by α, the motion of the "coupler" is not simple rotation about $\ell(\xi_1^A)$. (Indeed, its instantaneous center of rotation in the plane of Fig. 6 is obtained at the intersection of the perpendiculars to the translation directions through the base hinges.)

Figure 6 shows the equivalent mechanism when it is "folded" in a plane normal to $\ell(\xi_1^A)$. In Fig. 5, we see the equivalent linkage as a fourth leg of the PM, not affecting the mobility of the platform.

4 INVERSE POSITION KINEMATICS

In practice the PM is used as a regional manipulator (a 3-dof positioning device) with a (typically spherical) wrist attached to the end-effector at point S. This results in a combined hybrid manipulator, like the 5-dof Exechon PKMs, Figs. 1-2, and the 6-dof fixture agent X 150, Fig. 3. Let us denote the end-effector of this hybrid chain by *ee*.

Herein we assume that we have a 6-dof mechanism with a spherical wrist, centered at S. When solving the inverse kinematics of the hybrid tripod the first (easy) step is to obtain the coordinates of point S, which is a known point in the body *ee* whose location is given.

From this, one proceeds to solve the inverse kinematics of the 3-dof parallel tripod, given a point S of the 3-dof platform. The result is the three input parameters, i.e., the (actuated) joint variables of the prismatic joints.

To complete the inverse kinematics of the 6-dof hybrid manipulator, it remains to obtain the joint variables of the three actuated joints in the serial spherical wrist. This is obtained from the relative orientation of the hybrid-chain end-effector, *ee*, and the PM platform, *e*, by means of a standard Euler-angle calculation.

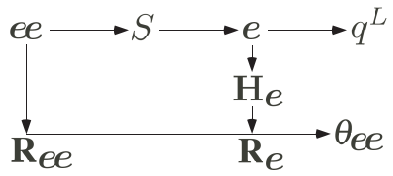

FIGURE 7: INVERSE KINEMATICS PROCEDURE.

The overall process of the inverse kinematics calculations is outlined in Fig. 7. In the figure, $\mathbf{H}_e$, $\mathbf{R}_e$ are the homogeneous and the rotation matrix of the PM platform, $\mathbf{R}_{ee}$ is the rotation matrix of the end-effector, while q^L and θ_{ee} are the actuated joint parameters of the PM and the spherical wrist, respectively.

Therefore, when solving the inverse kinematics of the parallel mechanism, what is normally given are the coordinates $[S_x, S_y, S_z]$ (in $(O\mathbf{i}_b\mathbf{j}_b\mathbf{k}_b)$) of a point S of the end-effector. (In particular, S may represent the center of a spherical wrist, as we have assumed.)

The solution of the inverse kinematics is easier if S is in the plane π_e^B through P_1^B orthogonal to $\mathbf{k}_S^B$. This does not represent a serious limitation because, in practical designs, π_e^B is a plane of symmetry of the end-effector, and the wrist center is placed in the plane of symmetry.

The coordinates of S in the end-effector frame $(P\mathbf{ijk})$ are $[h_x, 0, h_z]$.

In the following we provide the solution of the inverse kinematics for both cases of end-effector pose described by e or S. Section 4.1 presents the relations to calculate e from S. The inverse (calculation of S from e) is presented in Section 4.2 for completeness. The position and orientation of $(P\mathbf{ijk})$ with respect to $(O\mathbf{i}_b\mathbf{j}_b\mathbf{k}_b)$, as well as the inverse transformation, is calculated in Sections 4.3 and 4.4 as a function of e and S, respectively. The geometry parameters that are not calculated together with the transformations $(O\mathbf{i}_b\mathbf{j}_b\mathbf{k}_b) \mapsto (P\mathbf{ijk})$ and $(P\mathbf{ijk}) \mapsto (O\mathbf{i}_b\mathbf{j}_b\mathbf{k}_b)$ are obtained in Section 4.5. The procedure and the relations are the same whether the end-effector pose is described by e or S.

We use the base reference frame $(O\mathbf{i}_b\mathbf{j}_b\mathbf{k}_b)$. $P_1^A = [0, d^A, 0]$, $P_1^B = [d^B, 0, 0]$, $P_1^C = [0, d^C, 0]$, $\mathbf{k}_1^A = \mathbf{k}_1^C = \mathbf{j}_b$ are immediately calculated from the geometry of the mechanism.

4.1 Calculation of e from S

We calculate first the angles α_1 between $\overrightarrow{P_0S}$ and $-\mathbf{i}_b$, and α_2 between $\overrightarrow{P_0S}$ and π_α, with P_0 the projection of S on the line of ξ_1^A. It should be noted that points P, S, P_0 are all in π_e^B. We obtain: $c_{\alpha 1} = -S_x/t_0$, $s_{\alpha 1} = S_z/t_0$, $c_{\alpha 2} = \sqrt{t_0^2 - h_x^2}/t_0$, $s_{\alpha 2} = h_x/t_0$, with $t_0 = \sqrt{S_x^2 + S_z^2}$.

We have $\alpha = \alpha_1 + \delta_1^B \alpha_2$, where $\delta_1^B = \pm 1$ distinguishes between two possible feasible arrangements of the plane π_α and then of the end-effector. Two assembly modes of the mechanism

correspond to these two arrangements. We develop and obtain:

$$c_\alpha = (-\delta_1^B S_x \sqrt{t_0^2 - h_x^2} + h_x S_z)/t_0^2 \quad (2)$$

$$s_\alpha = (\delta_1^B S_z \sqrt{t_0^2 - h_x^2} + h_x S_x)/t_0^2 \quad (3)$$

From s_α and c_α we calculate $\mathbf{k}_2^A = \mathbf{k}_2^C = [s_\alpha, 0, c_\alpha]^T$.

The vector $\mathbf{k}_5^B$ is calculated from the cross product of $\overrightarrow{P_1^B S}$ and $\mathbf{k}_2^A$.

Then, s_β and c_β are obtained from the dot and cross products of $\mathbf{k}_5^B$ and $\mathbf{j}_b$: $s_\beta = -\delta_2^B S_y/\sqrt{t_6^2 + S_y^2}$, $c_\beta = \delta_2^B t_6/\sqrt{t_6^2 + S_y^2}$, with $t_6 = (\delta_1^B (t_0^2 - d^B S_x)\sqrt{t_0^2 - h_x^2} + d^B h_x S_z)/t_0^2$. $\delta_2^B = \pm 1$ distinguishes between two possible orientations of the end-effector with the same S and $\mathbf{k}_2^A$ and oppositely directed $\mathbf{k}_5^B$.

A compact expression of $\mathbf{k}_5^B$ is $\mathbf{k}_5^B = [-s_\beta c_\alpha, c_\beta, s_\beta s_\alpha]^T$.

The vector $\mathbf{e}_h$ is calculated as $\mathbf{k}_5^B \times \mathbf{k}_2^A$ yielding $\mathbf{e}_h = [-c_\beta c_\alpha, -s_\beta, c_\beta s_\alpha]^T$.

The coordinates of P in $(O\mathbf{i}_b\mathbf{j}_b\mathbf{k}_b)$ are obtained from the coordinates of S using $\mathbf{e}_h$ and $\mathbf{k}_2^A$: $P = [S_x, S_y, S_z]^T - h_x \mathbf{k}_2^A - h_z \mathbf{e}_h [S_x + h_z c_\beta c_\alpha - h_x s_\alpha, S_y + h_z s_\beta, S_z - h_z c_\beta s_\alpha - h_x c_\alpha]^T$.

The scalars h and l are, respectively, the projections of $\overrightarrow{OP}$ on $\mathbf{e}_h$ and $\mathbf{k}_5^B$:

$$h = \delta_2^B (S_y^2 + \delta_1^B t_6 \sqrt{t_0^2 - h_x^2})/\sqrt{t_6^2 + S_y^2} - h_z \quad (4)$$

$$l = s_\beta (-c_\alpha S_x + s_\alpha S_z) + c_\beta S_y \quad (5)$$

The three points, S, and its projections S_α on π_α and S_0 on $\ell(\xi_1^A)$, form a right triangle where t_0 and h_x are the lengths of the hypotenuse and of the short cathetus, respectively. For geometric reasons, $t_0^2 \geq h_x^2$ with $t_0^2 - h_x^2 = 0$ in configurations with S_α on the line of ξ_1^A. At these configurations, the pose of the end-effector is undetermined. A special case is $t_0^2 = 0$ (S on the line of ξ_1^A).

In every other case e can be computed.

For a generic S we have four possible poses of the end-effector corresponding to four different sets e. Figure 8 shows an example of four mechanism configurations with the same S. Note that, ignoring link interference, transition from one to the others is possible without disassembly.

4.2 Calculation of S from e

From s_α and c_α we calculate $\mathbf{k}_2^A = \mathbf{k}_2^C = [s_\alpha, 0, c_\alpha]^T$.
$\mathbf{k}_5^B = [-s_\beta c_\alpha, c_\beta, s_\beta s_\alpha]^T$.
$\mathbf{e}_h = \mathbf{k}_5^B \times \mathbf{k}_2^A = [-c_\beta c_\alpha, -s_\beta, c_\beta s_\alpha]^T$.

The coordinates of P can be calculated as $\overrightarrow{OP} = h\mathbf{e}_h + l\mathbf{k}_5^B$, with l the distance between P and the projection of O on π_h.

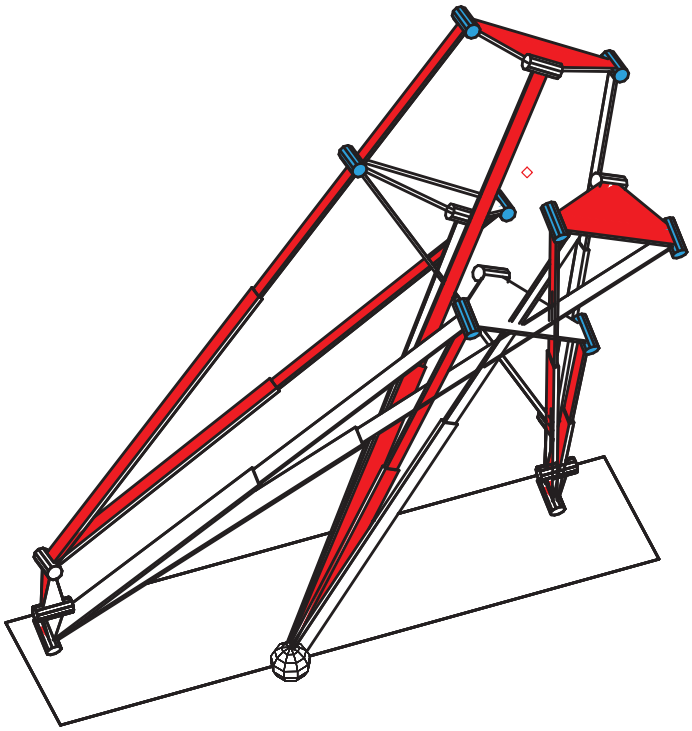

FIGURE 8: FOUR MECHANISM CONFIGURATIONS WITH SAME S

Imagine that the leg B is translated in direction $-\mathbf{k}_2^A$ so that P_5^B moves on P. Then, P_1^B moves to $\widetilde{P}_1^B$, and $\overrightarrow{O\widetilde{P}_1^B} = [d^B - p^B s_\alpha, 0, -p^B c_\alpha]^T$.

According to the architecture of the mechanism, $\overrightarrow{\widetilde{P}_1^B P} \perp \mathbf{k}_5^B$, therefore $\overrightarrow{\widetilde{P}_1^B P} \cdot \mathbf{k}_5^B = 0$. This equation is solved for l yielding $l = -d^B s_\beta c_\alpha$.

Substitution of the l formula yields: $\overrightarrow{OP} = [P_x, P_y, P_z] = [-c_\alpha (h c_\beta - c_\alpha d^B {s_\beta}^2, (-h - c_\alpha d^B c_\beta) s_\beta, s_\alpha (h c_\beta - c_\alpha d^B {s_\beta}^2)]$.

The coordinates of S are immediately calculated from P: $[S_x, S_y, S_z] = [P_x - h_z c_\beta c_\alpha + h_x s_\alpha, P_y - h_z s_\beta, P_z + h_z c_\beta s_\alpha + h_x c_\alpha]^T$.

Developing and simplifying: $[S_x, S_y, S_z] = [h_x s_\alpha, 0, +h_x c_\alpha] - (h + h_z)[c_\beta c_\alpha, s_\beta, -c_\beta s_\alpha] + (c_\alpha d^B s_\beta)[c_\alpha s_\beta, -c_\beta, -s_\alpha s_\beta]^T$.

Only one end-effector pose and S correspond to any given e.

4.3 Calculation of the transformations $(O\mathbf{i}_b\mathbf{j}_b\mathbf{k}_b) \mapsto (P\mathbf{ijk})$ and $(P\mathbf{ijk}) \mapsto (O\mathbf{i}_b\mathbf{j}_b\mathbf{k}_b)$ from e

We calculate the matrix associated to the homogeneous transformation of coordinates from $(O\mathbf{i}_b\mathbf{j}_b\mathbf{k}_b)$ to $(P\mathbf{ijk})$ as a function of e.

By definition $\mathbf{i} = \mathbf{k}_2^A$, $\mathbf{j} = \mathbf{k}_5^B$, $\mathbf{k} = \mathbf{e}_h$. Expressions for the coordinates of these vectors and of P in $(O\mathbf{i}_b\mathbf{j}_b\mathbf{k}_b)$ as functions of e are provided in Section 4.1.

In the matrix associated to the homogeneous transformation,

we write $\mathbf{k}_2^A$, $\mathbf{k}_5^B$, $\mathbf{e}_h$ as the rows in the rotation submatrix. The translation entries are $P_O \cdot \mathbf{k}_2^A = 0$, $P_O \cdot \mathbf{k}_5^B = -l = c_\alpha d^B s_\beta$, $P_O \cdot \mathbf{e}_h = -h$. We obtain:

$$\mathbf{H}_e = \begin{bmatrix} s_\alpha & 0 & c_\alpha & 0 \\ -s_\beta c_\alpha & c_\beta & s_\beta s_\alpha & c_\alpha d^B s_\beta \\ -c_\beta c_\alpha & -s_\beta & c_\beta s_\alpha & -h \\ 0 & 0 & 0 & 1 \end{bmatrix} \tag{6}$$

$\mathbf{H}_e$ transforms the coordinates of a point or a vector given in $(O\mathbf{i}_b\mathbf{j}_b\mathbf{k}_b)$ in the coordinates of the same point or vector in $(P\mathbf{ijk})$. For example $\mathbf{H}_e[S_x, S_y, S_z, 1] = [h_x, 0, h_z, 1]$ and $\mathbf{H}_e[e_{hx}, e_{hy}, e_{hz}, 0] = [0, 0, 1, 0]$.

The inverse transformation is:

$$\mathbf{H}_e^{-1} = \begin{bmatrix} s_\alpha & -s_\beta c_\alpha & -c_\beta c_\alpha & -c_\alpha c_\beta h - c_\alpha d^B {s_\beta}^2) \\ 0 & c_\beta & -s_\beta & -(h + c_\alpha d^B c_\beta) s_\beta \\ c_\alpha & s_\beta s_\alpha & c_\beta s_\alpha & s_\alpha c_\beta h - c_\alpha d^B {s_\beta}^2) \\ 0 & 0 & 0 & 1 \end{bmatrix} \tag{7}$$

For example $\mathbf{H}_e^{-1}[h_x, 0, h_z, 1] = [S_x, S_y, S_z, 1]$ and $\mathbf{H}_e^{-1}[0, 0, 1, 0] = [e_{hx}, e_{hy}, e_{hz}, 0]$.

4.4 Calculation of the transformations $(O\mathbf{i}_b\mathbf{j}_b\mathbf{k}_b) \mapsto (P\mathbf{ijk})$ and $(P\mathbf{ijk}) \mapsto (O\mathbf{i}_b\mathbf{j}_b\mathbf{k}_b)$ from S

We proceed as in Section 4.3 using the expressions in Section 4.1 to calculate $\mathbf{k}_2^A$, $\mathbf{k}_5^B$, $\mathbf{e}_h$, and P_O from the coordinates of S. Expressions for c_α, s_α, c_β, s_β as functions of the coordinates of S are also available. We collect the entries in the homogeneous matrix and obtain (with $t_8 = \sqrt{S_x^2 + S_z^2 - h_x^2}$):

$$\mathbf{H}_S = \begin{bmatrix} s_\alpha & 0 & c_\alpha & 0 \\ -s_\beta c_\alpha & c_\beta & s_\beta s_\alpha & -s_\beta \delta_1^B t_8 - c_\beta S_y \\ -c_\beta c_\alpha & -s_\beta & c_\beta s_\alpha & s_\beta S_y - c_\beta \delta_1^B t_8 + h_z \\ 0 & 0 & 0 & 1 \end{bmatrix} \tag{8}$$

For example $\mathbf{H}_S[S_x, S_y, S_z, 1] = [h_x, 0, h_z, 1]$ and $\mathbf{H}_S[e_{hx}, e_{hy}, e_{hz}, 0] = [0, 0, 1, 0]$.

The inverse transformation is:

$$\mathbf{H}_S^{-1} = \begin{bmatrix} s_\alpha & -s_\beta c_\alpha & -c_\beta c_\alpha & -c_\alpha(-c_\beta h_z + \delta_1^B t_8) \\ 0 & c_\beta & -s_\beta & S_y + s_\beta h_z \\ c_\alpha & s_\alpha s_\beta & c_\beta s_\alpha & s_\alpha(-c_\beta h_z + \delta_1^B t_8) \\ 0 & 0 & 0 & 1 \end{bmatrix} \tag{9}$$

For example $\mathbf{H}_S^{-1}[h_x, 0, h_z, 1] = [S_x, S_y, S_z, 1]$ and $\mathbf{H}_S^{-1}[0, 0, 1, 0] = [e_{hx}, e_{hy}, e_{hz}, 0]$.

4.5 Solution of the inverse kinematics

If the coordinates of S are assigned we follow the procedure in Section 4.1 and obtain c_α, s_α, c_β, s_β, h and $\mathbf{k}_2^A$, $\mathbf{k}_5^B$, $\mathbf{e}_h$, P (four sets identified by δ_1^B and δ_2^B).

If e is assigned we have immediately c_α, s_α, c_β, s_β, h and we calculate $\mathbf{k}_2^A$, $\mathbf{k}_5^B$, $\mathbf{e}_h$, P, S as in Section 4.2.

The other geometry parameters are calculated from c_α, s_α, c_β, s_β, h, if e or S are assigned.

$\mathbf{n}_{12}^A = [-c_\alpha, 0, s_\alpha]^T$.

The end-effector points P_4^A, P_5^B, P_4^C are calculated from P using $\mathbf{k}_2^A$, $\mathbf{k}_5^B$ and the geometry parameters p^A, p^B, p^C:

$$\overrightarrow{OP_4^L} = [c_\alpha(t_3 - p^L s_\beta - h^L c_\beta), p^L c_\beta - t_2 s_\beta - h^L s_\beta, \\ - s_\alpha(t_3 - p^L s_\beta - h^L c_\beta)]^T \tag{10}$$

$$\overrightarrow{OP_5^B} = [-t_1 s_\alpha + d^B - t_2 c_\alpha c_\beta, -t_2 s_\beta, t_2 s_\alpha c_\beta - t_1 c_\alpha]^T \tag{11}$$

where $L = A, C$, and $t_1 = d^B s_\alpha - p^B$, $t_2 = d^B c_\alpha c_\beta + h$, $t_3 = d^B c_\alpha - t_2 c_\beta$.

The expression q^B, the length of $\overrightarrow{P_1^B P_5^B}$, is $q^B = \sqrt{t_1^2 + t_2^2}$.

The vectors $\overrightarrow{OP_2^L}$, $L = A, C$, are immediately obtained from P_1^L: $\overrightarrow{OP_2^L} = [-\delta^L l_{12}^L c_\alpha, d^L, \delta^L l_{12}^L s_\alpha]^T$. The boolean parameters $\delta^L = \pm 1$, $L = A, C$, distinguish between the different working modes of the mechanism.

Finally, q^L, $L = A, C$, are calculated from the norm of $\overrightarrow{P_2^L P_4^L}$:

$$q^L = \sqrt{(t_3 - p^L s_\beta - h^L c_\beta + \delta^L l_{12}^L)^2 + (t_2 s_\beta - p^L c_\beta + h^L s_\beta + d^L)^2}$$

Figure 9 shows the four working modes of legs A and C. Transition between them is not possible without disassembly.

4.6 Numerical example

To conclude we provide a numerical example of the calculation of the inverse kinematics of the PM.

We assume the geometry in Tab. 1:

The given point S has coordinates $[0.02, 0.7, 1.02]$. This yields 4 solutions for the pose of the PM platform. They are illustrated in Fig. 8. For each of those poses, there are 4 solutions for the input parameters. The results are presented in Tab. 2.

A mathematical mockup of the Exechon tripod architecture has been created using Maple. The algorithms described in this section have been encoded and implemented on the mockup to automatically obtain the figures and the solutions of the example.

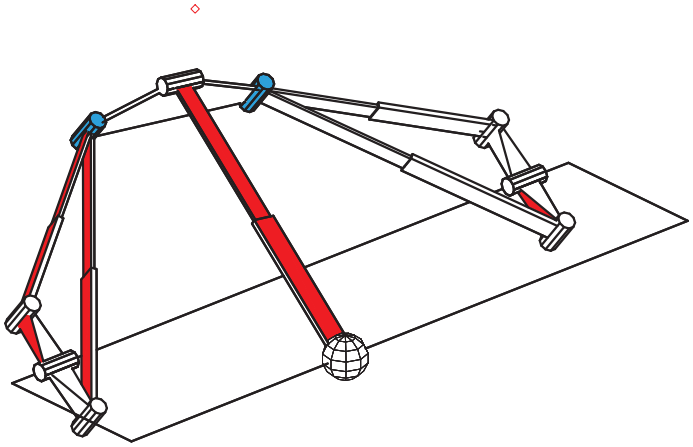

FIGURE 9: THE FOUR WORKING MODES OF LEGS A AND C

d^A	d^B	d^C	l_{12}^A	l_{12}^C	p^A
-0.4434	0.3455	0.7798	0.1023	0.1523	-0.1523
p^B	p^C	h^A	h^C	h_z	h_x
0.1324	0.2523	0.04	0.023	-0.2	0.2828

TABLE 1: NUMERICAL EXAMPLE GEOMETRY

$\delta_A, \delta_1^B, \delta_2^B, \delta_C$	s_α	c_α	s_β	c_β	h	q^A	q^B	q^C
$++++$	.9661	.2584	-.5476	.8367	1.403	.9122	1.492	1.633
$+++-$	.9661	.2584	-.5476	.8367	1.403	1.492	1.633	1.208
$++-+$	.9661	.2584	.5476	-.8367	-1.003	.8822	1.097	1.285
$++--$	.9661	.2584	.5476	-.8367	-1.003	1.160	1.097	1.285
$+-++$	-.9552	.2960	-.6234	-.7819	1.403	1.401	1.837	1.471
$+-+-$	-.9552	.2960	-.6234	-.7819	1.403	1.401	1.837	1.168
$+--+$	-.9552	.2960	.6234	.7819	-1.003	1.032	.8011	1.321
$+---$	-.9552	.2960	.6234	.7819	-1.003	.4967	1.032	1.321
$-+++$	.9661	.2584	-.5476	.8367	1.403	.9122	1.492	1.785
$-++-$	.9661	.2584	-.5476	.8367	1.403	1.492	1.208	1.785
$-+-+$	.9661	.2584	.5476	-.8367	-1.003	1.391	.8822	1.097
$-+--$	.9661	.2584	.5476	-.8367	-1.003	1.160	1.391	1.097
$--++$	-.9552	.2960	-.6234	-.7819	1.403	1.401	1.471	1.714
$--+-$	-.9552	.2960	-.6234	-.7819	1.403	1.401	1.168	1.714
$---+$	-.9552	.2960	.6234	.7819	-1.003	1.032	1.175	.8011
$----$	-.9552	.2960	.6234	.7819	-1.003	.4967	1.032	1.175

TABLE 2: NUMERICAL EXAMPLE SOLUTIONS

5 CONCLUSIONS

The analytical solution of the inverse kinematics of the Exechon 3-dof parallel mechanism has been presented for the first time. In addition, the inverse kinematics of the hybrid-geometry machines based on the tripod has been solved. The motion pattern of the 3-dof tripod has been described via a simple equivalent linkage.

ACKNOWLEDGMENT

We thank Exechon AB for the images of models X 700, X 300, and X 150. We acknowledge the support of the EU through the SwarmItFIX FP7 project.

REFERENCES

[1] Merlet, J.-P., 2000. *Parallel robots*. Kluwer.

[2] Schoppe, E., Ponish, A., Maier, V., Puchtler, T., and Ihlenfeldt, S., 2002. "Tripod machine skm 400 design, calibration and practical application". In Parallel Kinematics Seminar, PKS2002, Chemnitz, Germany, pp. 579–594.

[3] Wahl, J., 2000. *Articulated tool head*. Patent WO 0025976.

[4] Chang, T.-H., Inasaki, I., Morihara, K., and Hsu, J.-J., 2000. "The development of a parallel mechanism of 5-dof hybrid machine tool". In PKM International Conference, Ann Arbour, Michigan, pp. 79–86.

[5] Saenz, A., Collado, V., Gimenez, M., and San Sebastian, I., 2002. "New automationsolutions in aeronautics through parallel kinematic systems". In Parallel Kinematics Seminar, PKS 2002, Chemnitz, Germany, pp. 563–578.

[6] Kong, X., and Gosselin, C., 2007. *Type Synthesis of Parallel Mechanisms*. Springer.

[7] Neumann, K.-E., 2006. *Parallel Kinematic Machine with an active measuring system*. Patent WO2006062466. Applicant: Exechon AB, Neumann, K.-E., Sweden.

[8] Neumann, K.-E., 1986. *Robot*. Patent SE8502327. Applicant: Neos Products, Sweden.

[9] Molfino, R., Zoppi, M., and Zlatanov, D., 2009. "Reconfigurable swarm fixtures". In ASME/IFToM International Conference on Reconfigurable Mechanisms and Robots, London.